Advances in Geosciences Vol. 15: Planetary Science (2007) Eds. Anil Bhardwaj *et al.* © World Scientific Publishing Company

THE MIP EXPERIMENT OF THE ROSETTA ORBITER: A MUTUAL IMPEDANCE PROBE FOR WAVES AND PLASMAS DIAGNOSIS

JEAN-GABRIEL TROTIGNON*,§, XAVIER VALLIERES*, DOMINIQUE LAGOUTTE*, SANDRINE GRIMALD*, JEAN-PIERRE LEBRETON† and PATRICK ROBERT‡

* Laboratoire de Physique et Chimie de l'Environnement et de l'Espace Centre National de la Recherche Scientifique Orléans University, 3A, Avenue de la Recherche Scientifique F-45071 Orléans cedex 02, France

 † Solar System Division, ESA/ESTEC NL-2200 AG Noordwijk, The Netherlands

[‡]Laboratoire de Physique des Plamas 10-12 Avenue de l'Europe, F-78140 Vélizy, France [§] Jean-Gabriel. Trotignon@cnrs-orleans.fr

The ROSETTA orbiter and lander will rendez-vous with the comet 67P/ Churyumov-Gerasimenko round 2014 and study it for a period of nearly 2 years. A plasma and wave package, the ROSETTA Plasma Consortium, RPC, is part of the orbiter payload. Five sensors will determine the development and activity of the comet during its approach to the Sun. One of these instruments, the Mutual Impedance Probe, MIP, has to measure the electron density and temperature in the cometary coma, and in particular, inside the contact surface. Furthermore, the MIP will determine the bulk velocity of the ionized outflowing atmosphere, define the spectral distribution of natural waves from $7\,\mathrm{kHz}$ to $3.5\,\mathrm{MHz},$ and monitor dust and gas activities around the nucleus. The MIP instrumentation has been developed by the LPC2E of CNRS (Orléans, France) and the ESTEC/RSSD of ESA (Noordwijk, The Netherlands). To reach the comet, the spacecraft must undergo four planet gravity assistances. The first one, an Earth flyby, occurred in early March 2005. At the closest approach, on 4 March at 22:09 UT, ROSETTA passed at about 1950 km over the Pacific Ocean just west of Mexico. During this event, valuable observations have actually been made by the MIP in the Earth's plasmasphere, a high electron-density region dominated by the Earth's magnetic field. The MIP principle of measurements, the instrument design, and the scientific results obtained in the Earth's plasmasphere are presented.

J.-G. Trotignon et al.

1. Introduction

In November 1993, the European Space Agency's Science Programme Committee (SPC) approved the ROSETTA mission, a comet chaser whose prime objective is to study the origin of comets, the relationship between cometary and interstellar material, and its implication with regard to the origin of the Solar System. Among the investigations to be made in support of this objective is the study, in situ, of the plasma and wave environment of a comet and the interaction with the dust and gas materials, from the onset of activity beyond 3.5 AU to perihelion. This goal was set by the ROSETTA Science Team for a restricted plasma package aboard the ROSETTA Orbiter. Five sensors were selected to achieve this aim. The need for scientific and technical coordination and optimization of spacecraft resources then led to the formation of the ROSETTA Plasma Consortium (RPC) which was finally approved by the SPC, as part of the ROSETTA's payload, on 2–3 June 1997.

The ROSETTA mission will therefore allow plasma physicists to investigate for the first time the innermost regions of the coma, and in particular the region inside the contact surface (Fig. 1) that was only

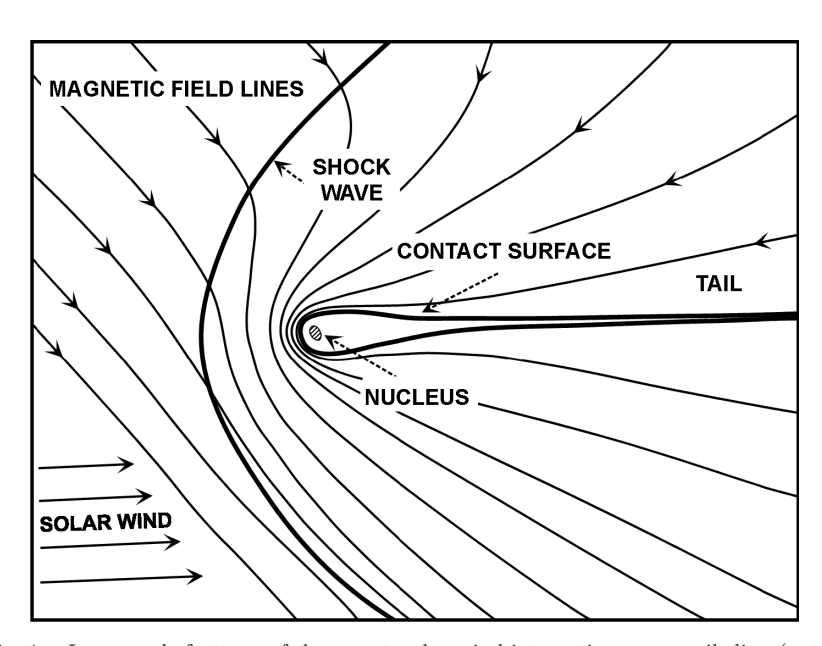


Fig. 1. Large-scale features of the comet–solar wind interaction near perihelion (not to scale).⁴ The inward pressure exerted by the solar wind flow is balanced by the outward pressure exerted by cometary gases.

skimmed by Giotto. The contact surface forms where the solar wind pressure, which is mostly magnetic outside the contact surface, equals the cometary thermal plasma pressure, whenever the gas production rate is sufficient. This boundary also prevents the inner part of the coma being reached by the interplanetary magnetic field, perturbed by the presence of the extremely large cometary environment. Strong asymmetries will occur if the gas is produced in a few active regions, as found in the Vega and Giotto observations of comet Halley's nucleus. RPC investigations will therefore allow the local and temporal effects of nucleus activity on coma structure and dynamical behavior to be described and understood.⁴

The Mutual Impedance Probe (MIP), part of RPC, will measure the aeronomical parameters, electron density and temperature, as well as plasma flow velocity in the inner coma. In addition, it will investigate natural waves in the 7 kHz to 3.5 MHz frequency range and monitor the dust and gas activity of the nucleus.

The purpose of this chapter is to present the MIP experiment in context. A brief summary of the ROSETTA mission and RPC consortium is therefore given in Sec. 2. Section 3 then deals with the scientific objectives, instrumentation, and frequency response modeling of the MIP. Finally, Sec. 4 shows the observations made in the Earth's plasmasphere during the first Earth swingby.

2. The ROSETTA Mission and RPC Plasma Consortium

2.1. The ROSETTA mission

ESA's comet chaser, ROSETTA,¹⁻³ comprises an orbiter and a small lander, PHILAE. Each of these carries a large complement of scientific experiments to study comet 67P/Churyumov-Gerasimenko from August 2014 to the end of 2015. ROSETTA was launched as flight 158 on 2 March 2004 by an Ariane-5G rocket from Kourou, in French Guiana. To leave the inner Solar System behind and set course for the distant comet at about 5.25 AU, ROSETTA has to receive gravity assists three times from Earth (in March 2005, November 2007, and November 2009) and once from Mars (in February 2007). During its long trek, ROSETTA will make two excursions into the asteroid belt, between the orbits of Mars and Jupiter, and will flyby 2867-Steins and 21-Lutecia asteroids, in September 2008 and July 2010, respectively.

J.-G. Trotignon et al.

2.2. The RPC plasma consortium

Five instruments were selected to measure the ion and electron distribution functions, ion composition, electron density and temperature, plasma drift velocity, magnetic field, and 0–3.5 MHz natural waves. The wide range of plasma parameters expected over the mission as a whole requires the instrument capabilities to be as comprehensive as possible. Moreover, to conserve the spacecraft's mass and power resources, and to provide a single interface to the spacecraft, the ROSETTA Plasma Consortium (RPC) was formed,⁴ covering the five sensors, the common interface (Plasma Interface Unit, PIU),⁵ and a ground support equipment (Fig. 2). The MIP instrument is described in Sec. 3, while the four others are briefly presented hereby.

The Ion Composition Analyzer (ICA)⁶ measures the distribution function of positive ions. The instrument resolves the 3D velocity distribution of cometary and solar wind ions, with a mass resolution high enough to resolve the major species such as protons, helium, oxygen, molecular ions, and heavy-ion clusters (dusty plasma). The 2.0 kg instrument consists of an electrostatic arrival angle filter, an electrostatic energy filter, and a magnetic momentum filter. Particles are detected using a large diameter (100 mm diameter) microchannel plate and a 2D anode system. ICA has its own processor for data reduction/compression and formatting.

The Ion and Electron Sensor (IES)⁷ consists of two electrostatic analysers, one each for electrons and ions, sharing a common entrance aperture. The charged particle optics for IES employ a toroidal top-hat geometry along with electrostatic angle deflectors to achieve an electrostatically scanned field of view of $90 \times 360^{\circ}$. The large field of view will be used to measure the ions and electrons of the solar wind, ions and electrons in the coma, and sputtered ions and photoelectrons generated on the cometary nucleus.

The primary objectives of the dual Langmuir probe (LAP)⁸ are to study the plasma density, temperature, and flow velocity. It comprises two spherical sensors mounted on the tips of deployed booms. The sensors can be swept in potential to measure the current–voltage characteristic for information on the electron number density and temperature. The probes can be held at a fixed bias potential to measure plasma-density fluctuations from the plasma structures, and to determine the plasma flow velocity by a time-of-flight analysis of the signals from the two probes. Close coupling with the neutral gas is expected in the inner coma; so, the measurement will provide information on the neutral gas flow.



Fig. 2. The ROSETTA plasma consortium is composed of five instruments and a common interface to the spacecraft.

J.-G. Trotignon et al.

The MAG⁹ experiment will measure the magnetic field in the interaction region between the solar wind plasma and the comet. It consists of two ultralight (about 28 g each) triaxial fluxgate magnetometer sensors: one mounted close to the tip of a boom pointing away from the cometary nucleus and one about 30 cm closer to the bus. Two sensors are required for redundancy and to minimize the influence of the spacecraft's magnetic field. The measurement range is $\pm 6384\,\mathrm{nT}$ in steps of $\pm 0.032\,\mathrm{nT}$. They will be operated with a high-time resolution of about 50 vectors/s, thus achieving a bandwidth of 0–25 Hz. This performance will allow detailed analysis of magnetic field variations. MAG is also designed to measure the possible remanent magnetic field of the nucleus, in close cooperation with the ROMAP lander magnetometer.

3. The Mutual Impedance Probe, MIP

3.1. The MIP scientific objectives

The scientific objectives of the Mutual Impedance Probe $(MIP)^{10}$ are closely related to the cometary atmospheric ionization and thermalization processes, and the nucleus dust and gas activities. It will determine the density and temperature of the thermal electron population and measure one component of the bulk velocity of the ionized outflowing atmosphere. MIP will also characterize the spectral distribution of natural plasma waves in the 7 kHz to $3.5\,\mathrm{MHz}$ frequency range and sense the impacts of dust particles.

3.2. The MIP instrumentation

The MIP instrument 10 comprises a lightweight electrical sensor made of carbon fiber and an electronics board. The latter is for experiment managing, input/output data handling, and signal processing in the $7\,\mathrm{kHz}$ - $3.5\,\mathrm{MHz}$ range.

The comb-shaped sensor unit consists of two receiving and two transmitting electrodes supported by a 1-m long cylindrical bar. The receiving electrodes are at the ends of the bar in order to maximize the effective length of the antenna for natural wave measurements (in passive mode, when no signals are transmitted). The electrodes are small metallic cylinders mounted at stud tips. The measured voltages are driven into high input impedance preamplifiers, located inside the studs that support the receiving electrodes, through 0.12 pF capacitors. In this way, the

MIP performance has the virtue of being independent of the chemical composition and the photoemissive properties of the electrodes, and it is immune from contamination by dust and ice deposits. The extremely low energetic plasmas expected within the contact surface can therefore be explored.

The electronics board houses both analog and digital components. The former includes a differential amplifier, an anti-aliasing filter, and an 8-bit analog-to-digital converter. The latter is structured around a digital signal processor (ADSP2100A) to compute Fast Fourier Transforms and two field programmable gate arrays (FPGA) to host the MIP digital synthesizer and to manage interfaces to the PIU.

3.3. The MIP principle of measurements

The MIP principle of measurement consists in determining the mutual impedance between a transmitting Hertz dipole and a receiving one.^{11,12} The transmitting electrodes are excited from a constant current source, at given frequencies lying in a range that includes the plasma frequency Fpe ($Fpe = 9 \sqrt{Ne}$, where the electron density Ne is expressed in cm⁻³, Fpe in kHz), while the receiving electrodes are connected to a voltmeter with very high input impedance.

Both the imaginary and real parts of the mutual impedance Z=V/I depend on dielectric properties of the plasma in which the electrodes are immersed. Moments of the thermal electron distribution function, such as the density, temperature, and drift velocity may therefore be deduced from the frequency response (also called transfer impedance or mutual impedance) of the MIP. Whenever the magnetic field is low, i.e. the electron cyclotron frequency Fce ($Fce=28\,B$, where B is expressed in nT and Fce in Hz) is much lower than Fpe, the frequency response exhibits one resonance peak near Fpe, from which the total plasma density Ne is derived, and an interference pattern¹³ associated with the propagation of thermal waves which gives the plasma Debye length λ_D . This interference pattern, which results from the beat of standing and propagating signals generated by the transmitting electrodes, is sensitive to Doppler effects, and the electron drift velocity may thus be determined.

In addition, since λ_D is a function of both Ne and the thermal electron temperature Te, a direct measurement of Te becomes possible ($\lambda_D = 6.9$ (Te/Ne)^{1/2}, where λ_D is expressed in cm, Te in °K, and Ne in cm⁻³). Conversely, if Fce and Fpe are of the same order of magnitude, resonances

J.-G. Trotignon et al.

330

at the upper-hybrid frequency Fuh ($Fuh = (Fpe^2 + Fce^2)^{1/2}$) and Bernstein frequencies 14,15 FQn, and anti-resonances at Fce and harmonics nFce are currently observed. In the latter case, the magnetic field strength may therefore be deduced (see Sec. 4).

3.4. The MIP short and long Debye length modes

As long as transmitting electrodes are placed at large enough distances from the receiving ones, potential difference V measured between the receiving electrodes, on open circuit, is independent of perturbations due to the ion sheaths that form around the electrodes. The transmitter–receiver distance has thus to be larger than twice the plasma Debye length. As this distance is $40\,\mathrm{cm}$, only plasmas with a Debye length lower than $20\,\mathrm{cm}$ should be properly measured with the MIP sensor alone (it is the so-called short Debye length mode, SDL).

To overshoot this limit, the long Debye length mode (LDL) has been designed. In this mode, the LAP 2 spherical Langmuir probe that is located at about 4 m from the MIP sensor will be used as a transmitter, and the MIP receiving dipole as a receiver (Fig. 3). In this way, plasmas with Debye lengths up to 2 m may be investigated.

3.5. Numerical modeling of the MIP frequency response

The frequency response of the MIP should be a function of the ambient magnetic field, densities, velocity distributions, and collision rates of charged particles. As far as a suitable theory or modeling is available, a comprehensive investigation of encountered plasmas may be done. ^{11,16} A modeling based on the surface charge distribution method (SCD) in quasistatic conditions has therefore been developed to predict the MIP frequency response at comet 67P/Churyumov-Gerasimenko. This model relies on the following assumptions: the antenna is immersed in homogenous and isotropic (unmagnetized) Maxwellian plasmas with no drift. The working frequency is around the plasma frequency so that only electrons are considered. The size of the antenna is much smaller than the wavelength of electromagnetic waves, i.e. the quasi-static approximation applies. The electron population is supposed to be thermalized and the contribution of suprathermal populations is negligible. This is particularly valid below the comet's contact surface.

According to the SCD method, the conductive surfaces of the antenna and spacecraft structures, including the solar panels, are first split into

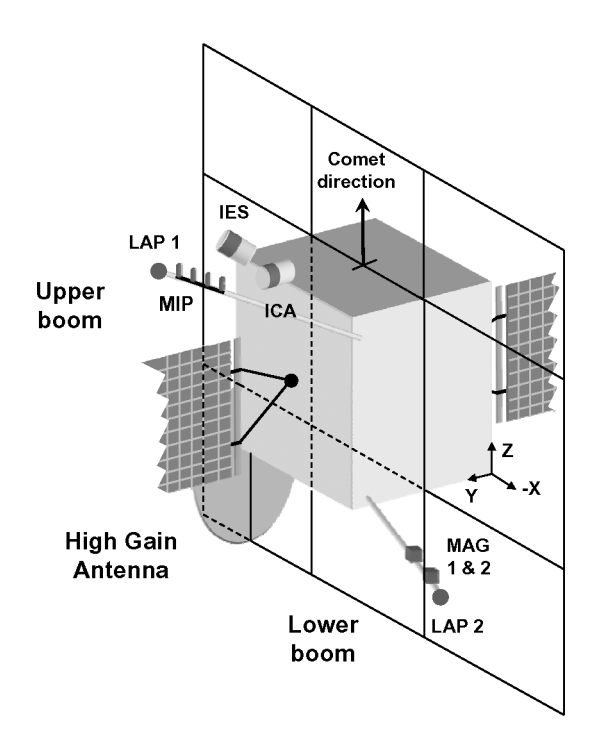


Fig. 3. MIP and LAP 2 sensors are used in the MIP Long Debye Length mode.

finite elements, each of them acting as a point-pulsating charge. In other words, their size is smaller than the ambient plasma Debye length, and the surface-charge distribution can be considered as uniform. Then, the kinetic approach proposed by Béghin and Kolesnikova is used.^{17,18} It consists in solving a linear set of equations where the finite element charges and the voltages of conductive surfaces are the unknown quantities. In these equations, point charge electrostatic potentials are expressed under the form of a series expansion.¹⁹ Considering that the total charge is equal to zero, the system of equations is closed and finally solved in inverting a quite large complex matrix.

As a matter of fact, two different approaches have been used to model the MIP frequency response depending on the expected plasma Debye lengths. 20,21 For plasmas with a short Debye length compared with the antenna length, i.e. $\lambda_D < 20\,\mathrm{cm}$, only the MIP sensor surface elements are taken into account, and a $2\lambda_D$ wide ion sheath is considered (SDL working mode of MIP). Conversely, for long Debye length

J.-G. Trotignon et al.

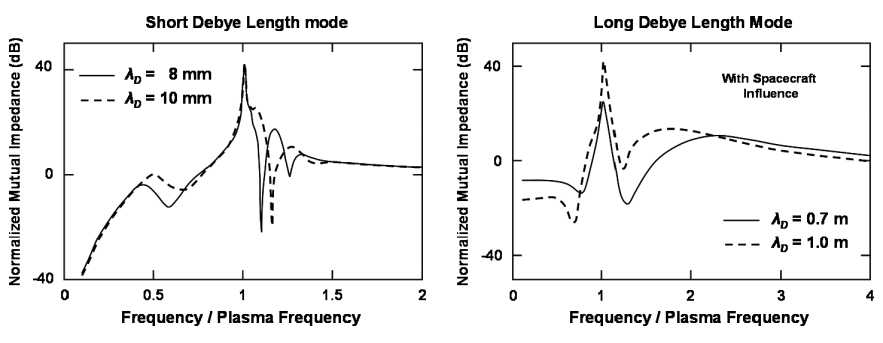


Fig. 4. Modeling of the MIP frequency response in SDL (left panel) and LDL (right panel) modes for different plasma Debye lengths. The ROSETTA structures are taken into account in LDL.

plasmas, $20\,\mathrm{cm} < \lambda_D < 2.5\,\mathrm{m}$, the conductive structures of the $2.8 \times 2.1 \times 2.0\,\mathrm{m}$ spacecraft and the two enormous, each $32\,\mathrm{m}^2$ in area, solar panels can no longer be ignored (LDL mode). Some results of the SDL and LDL modelings are shown in Fig. 4.

4. MIP Measurements in the Earth's Plasmasphere

En route to Comet 67P/Churyumov-Gerasimenko, the ROSETTA spacecraft underwent its first planet gravity assistance in early March 2005. At the closest approach, on 4 March 2005, at 22:09:16 UT, ROSETTA passed at about 1955 km over the Pacific Ocean just west of Mexico (Fig. 5).

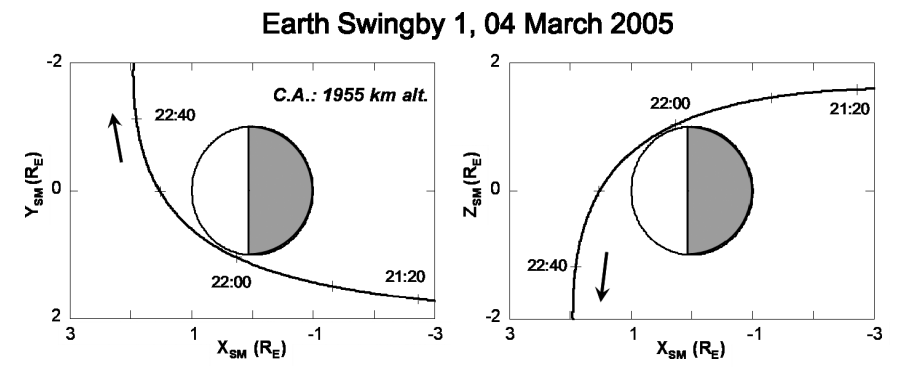


Fig. 5. ROSETTA trajectory, in solar magnetic coordinates, on 4 March 2005 during the first Earth's gravity assist. The Z-axis is parallel to the north magnetic pole and the Y-axis is perpendicular to the Earth–Sun line toward dusk. ROSETTA passed at about 1955 km over the Pacific Ocean just west of Mexico.

The three-tonne vehicle flew over the Earth with a relative velocity of a little bit more than $10\,\mathrm{kps}$ (38,000 kph). It was the closest-ever Earth flyby made by an ESA's spacecraft.

The mutual impedance probe, MIP, and the four other instruments of the ROSETTA Plasma Consortium, RPC, were switched on during the event. Calibration and general testing were the main objectives, nevertheless valuable observations of the Earth's space environment have actually been made, in particular in the plasmasphere. It is a vast toroidal region of cool but dense plasma of ionospheric origin, which is dominated by the Earth's magnetic field and corotates with the planet.

Four individual spectra measured by MIP in the Earth's plasmasphere have been chosen to be displayed in Fig. 6. As expected, the electron gyrofrequency Fce and its harmonics nFce are seen as anti-resonances, while the plasma frequency Fpe, the upper-hybrid frequency Fuh, and Bernstein frequencies FQn appear as resonances. When looking at these spectra,

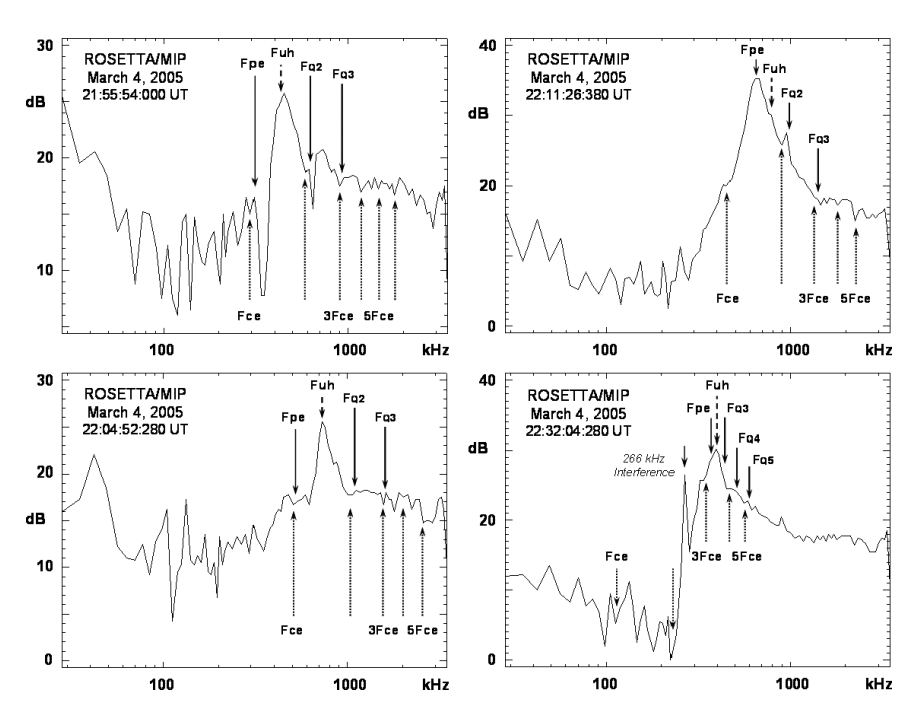


Fig. 6. Typical spectra measured in the Earth's plasmasphere by the MIP mutual impedance probe onboard the ROSETTA spacecraft. Anti-resonances arise at the electron gyrofrequency Fce and harmonics nFce, while the plasma frequency Fpe, upperhybrid frequency Fuh, and Bernstein's frequencies FQn appear as resonances.

one after the other, it becomes clear, that identifying such signatures is sometimes tricky, in particular when the signal to noise ratio is small and/or the Debye length is quite large compared with the antenna length. Another limitation comes from the frequency resolution which is of 7 kHz between 28 kHz and 224 kHz, 14 kHz between 224 kHz and 448 kHz, 28 kHz between 448 kHz and 896 kHz, 56 kHz between 896 kHz and 1792 kHz, and finally 112 kHz from 1792 kHz to 3472 kHz. There are different ways to overcome these difficulties; the spectra may be averaged in order to reduce the noise level, and the resonances and anti-resonances may be more easily identified, by continuity, in looking at their time variations. This is illustrated in Fig. 7, where the passive and active measurements are shown on the left- and right-hand sides, respectively. The time is running from top to bottom and each spectrum is an average of five consecutive spectra, each

Earth Swingby 1, ROSETTA/MIP, March 4, 2005

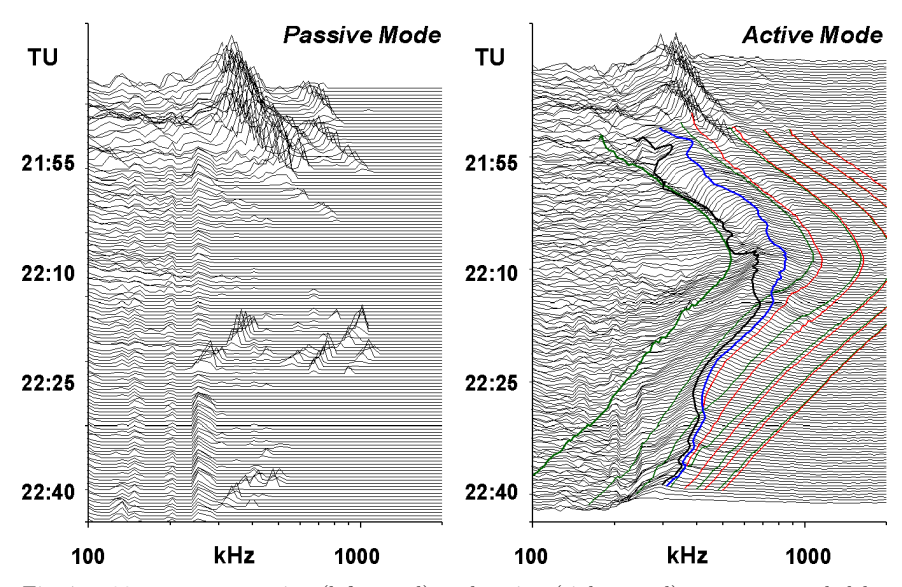


Fig. 7. 20-s average passive (left panel) and active (right panel) spectra recorded by the ROSETTA/RPC/MIP instrument during the first Earth flyby on 4 March 2005. The left panel shows kilometric continuum radiations round 21:45, 22:15, and 22:35 UT, at about 40°, 12°, and -24° magnetic latitude. The low-frequency vertical structures seen on both panels are instrument interferences. Characteristic plasma frequencies, Fce (thick green line), nFce (thin green lines), Fpe (thick black line), Fuh (thick blue line), and FQn (thin red lines) are superimposed on the active measurements of the mutual impedance modulus.

of 4-s duration. The green, black, blue, and red traces are, respectively, the identified nFce (n=1 to 6), Fpe, Fuh, and FQn (n=2 to 5) structures. These structures may also be hidden by strong wave emissions; this is unfortunately the case before 21:40 UT when kilometric continuum radiations were detected. These waves are shown on the left-hand panel of Fig. 7, at the top. The analysis of these emissions is out of the scope of this chapter (they will indeed be discussed in a future publication), but we can say that they have currently been observed, in particular by Geotail as fine structures of narrow-bandwidth linear features that slowly drift in frequency, in the $100\,\mathrm{kHz}$ to $800\,\mathrm{kHz}$ frequency range, i.e. almost in the same range as auroral kilometric radiations. ^{22,23} A distinctive feature of the waves observed onboard ROSETTA, is that we are here in the evening sector at 18-21 magnetic local time and quite far from the magnetic equator, at $30^\circ-40^\circ$ magnetic latitude.

As shown in Fig. 8, both the phase and modulus of the MIP frequency response contain information on the plasma frequency characteristics. They are shown, respectively, in the top and bottom panel, with relative value color-coded. Identified plasma frequencies are superimposed as color lines. The electron cyclotron frequency (Fce) and its harmonics (nFce) are green in the phase panel (top) and white in the modulus panel (bottom). Similarly, the white (top) and black (bottom) lines represent the plasma frequency (Fpe) while the upper hybrid frequency (Fuh) is the blue trace for both the phase and modulus. Finally, the red lines point out the Bernstein's frequencies (FQn). During this one-hour period, ROSETTA moved from the nightside to the dayside of the Earth's plasmasphere at geocentric distances between 1.3 R_E, at closest approach, and 2.5 R_E, at extremities. Let us also note that a quite large magnetic latitude interval was covered, from 36.1° to -28.2°, and the magnetic equator was crossed a little bit after 22:20 UT, around which the most intense values of the antenna impedance modulus were actually registered. As said above, the narrowbanded and very intense structures extending from 250 kHz to over 600 kHz are kilometric continuum radiations; they are seen, both on the phase and modulus from the beginning of the plots to 21:53 UT.

Fce and Fpe values predicted by, respectively, the Tsyganenko²⁴ T89 magnetosphere and Gallagher $et~al.^{25}$ plasmasphere models have been compared with those measured by MIP. Figure 9 shows that Fce, and hence the magnetic field strength, deduced from the MIP data does not significantly differ from the T89 one. The thin solid line is indeed close to the dashed line, apart from a few overestimated values between

J.-G. Trotignon et al.

Earth Swingby 1, ROSETTA/MIP, March 4, 2005

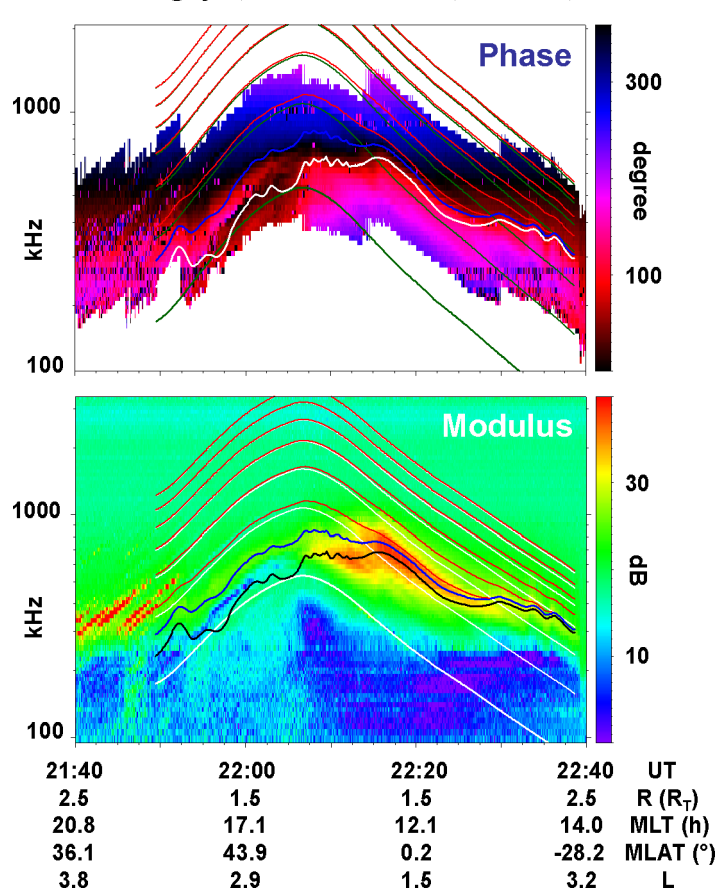


Fig. 8. From top to bottom: frequency versus time phase and modulus of the mutual impedance of the MIP electric antenna in the Earth's plasmasphere. In the bottom panel, the derived Fpe, Fuh, and FQn resonances are respectively shown as thick black, thick blue, and thin red lines, while the thick and thin white curves denote nFce (anti-resonances). For convenience, the same characteristic plasma frequencies are plotted in different colors in the phase panel. Intense kilometric continuum emissions actually screened the resonance and anti-resonance signatures before 21:50 UT. The largest values of the mutual impedance modulus were detected round 22:20 UT near the magnetic equator crossing.

21:49 and $21:52\,\mathrm{UT}$ (where strong natural waves occurred). It is worth noting that these values are also in a fairly good agreement with the MAG magnetometer measurements. If we now look at Fpe, and hence the plasma density, the MIP determinations (thick dashed line with diamonds) are of

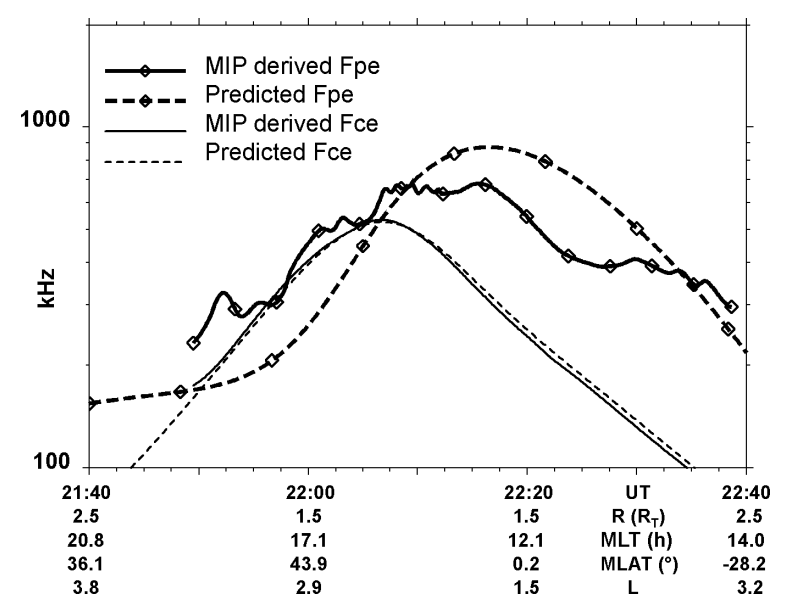


Fig. 9. Electron gyrofrequencies Fce derived from the MIP observations in the Earth's plasmasphere are consistent both with the values predicted by the T89 Tsyganenko's model²⁴ and the MAG magnetometer measurements. Gallagher $et\ al.^{25}$ predicted plasma frequencies are not drastically different from the MIP determinations.

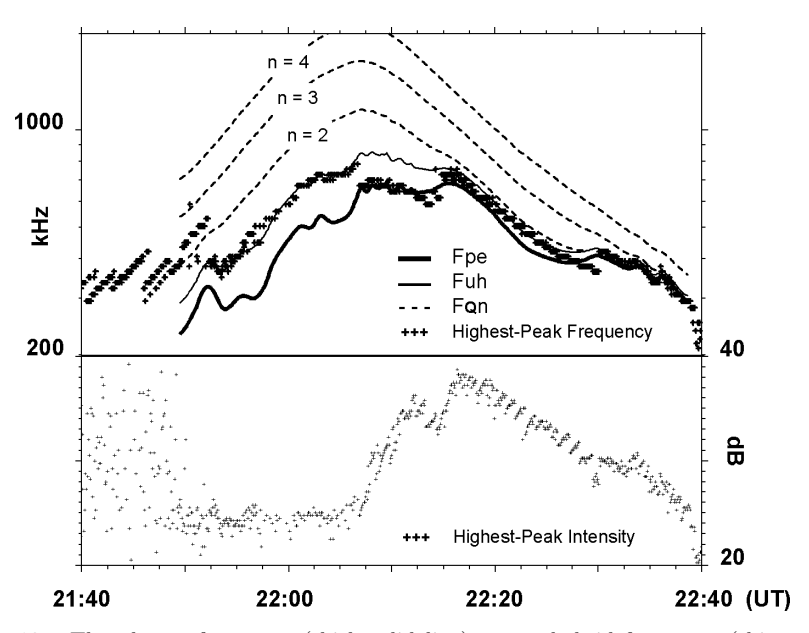
the same order of magnitude as predictions (thick solid line with diamonds), but they are also unsurprisingly very different from the empirical model which can no longer reproduce density profiles, for example, for any of the geomagnetic activities.

The Debye length, from which the thermal electron temperature is deduced, decreased from 17.4 cm at 21:40 UT to 6.6 cm at 22:20 UT before increasing up to 19 cm at 22:40 UT. It was therefore lower than 20 cm, which is the upper limit for the measurements to be made in the LDL working mode. These values are consistent with those predicted by Titheridge. An accurate temperature profile will be produced in the next future in cooperation with the LAP Langmuir probe experimenters. It is indeed not easy to obtain a precise estimate in the absence of a reliable modeling of strongly magnetized plasmas.

Crosses in the top and bottom panels of Fig. 10 point out, respectively, the frequency at which the MIP frequency response modulus reached its maximum and the amplitude of this maximum in the time interval ranging from 21:40 to 22:40 UT. Also plotted at the top are the plasma frequency,

May 15, 2009 15:7

 $9in \times 6in$



The plasma frequency (thick solid line), upper-hybrid frequency (thin solid line), and Bernstein's frequencies (dashed lines) are displayed in the top panel, in addition to the frequency at which the mutual impedance modulus of the MIP electric antenna reaches its maximum (crosses). The intensity of these extremes is shown below. Intense kilometric continuum radiations do not allow resonances and anti-resonances to be detected below $21:50\,\mathrm{UT}$. The highest-peak frequency sometimes takes place at the plasma frequency, the upper-hybrid frequency, or between these two characteristic plasma frequencies.

upper-hybrid frequency, and the three first Bernstein's frequencies identified in the MIP data during the crossing of the Earth's plasmasphere by the ROSETTA spacecraft, on 4 March 2005. The maxima detected between 21:40 and 21:53 UT do not correspond to any of the characteristic plasma frequencies but actually to the kilometric continuum radiations already mentioned. The high level of the waves, which can be as high as the highest plasma resonance seen round 22:20 UT, indeed makes the plasma resonances screened. From 21:53 to 22:07 UT, the spectrum maxima follow quite well the upper-hybrid frequency, as the plasma frequency remains close to the electron cyclotron frequency as shown in Fig. 9. A sudden drop then occurs at 22:07 UT, and crosses are now superimposed on the plasma frequency. In the same time, the plasma frequency varies from Fce to 2Fce (Fig. 9). Two other breakdowns actually happen at 22:15 and 22:30 UT, exactly when the plasma frequency becomes higher than the second and then the third gyroharmonics (see Fig. 9). The consequence of this is that taking the highest-peak frequency in each spectrum as the plasma frequency, from which the plasma density is directly derived, entails an error in the density determination which increases when Fpe/Fce decreases.

5. Conclusion

The ROSETTA mission, which is comprised of an orbiter and the PHILAE lander, will investigate for the first time in orbit a comet and follow it along its trajectory around the Sun, from at least 3.5 AU (in August 2014) to perihelion (in August 2015). Along its long trek to the comet, ROSETTA will undergo not less than four planetary gravity assists and will visit two belt asteroids. An extended monitoring of the comet is then anticipated until the end of 2015. As part of the orbiter payload, five instruments and a common interface unit compose the RPC ROSETTA plasma consortium whose main scientific objective is to study structure and dynamics of the interaction between the comet 67P/Churyumov-Gerasimenko environment and the solar wind. The MIP mutual impedance probe is one of these five instruments. It measures the electrical coupling between two transmitting cylindrical electrodes and two receiving ones supported by a 1-m long conductive bar, from which the first moments of the thermal electron distribution function, density, temperature, and drift velocity, are derived. In addition, the electric component of natural waves will be measured in a 7 kHz-3.5 MHz frequency range, and the dust and gas activities monitored all along the comet trajectory.

After a commissioning period of a few months after the 2 March 2004 launch from Kourou, the MIP experiment has been declared fully operational. Numerical modelings of the MIP working modes have also confirmed that the mutual impedance technique is well suited for investigating comet 67P/C-G plasma environment, in particular inside the contact surface, where the interplanetary magnetic field does not penetrate. Valuable scientific measurements were finally made during the first planetary gravity assist; it was in the Earth's plasmasphere on 4 March 2005. Both the magnetic field strength and the total plasma density have been measured and compared with models. The Debye length determination, and hence the temperature determination, will require additional efforts in cooperation with the LAP Langmuir probe experimenters. Only a crude estimate may indeed be made in the absence of a reliable modeling of a strongly magnetized plasma, which is fortunately

J.-G. Trotignon et al.

not the case of a comet-ionized environment. Finally, very intense kilometric continuum radiations were recorded, and they are located at unusual magnetic latitudes.

References

- J. Ellwood, G. Schwehm, The ROSETTA Project Team and P. Bond, ESA Bull. 117 (2004) 5.
- C. Berner, L. Bourillet, J. van Casteren, J. Ellwood, M. Kasper, P. Kletzkine,
 R. Schulz, G. Schwehm, M. Warhaut and P. Bond, ESA Bull. 112 (2002) 10.
- K. H. Glassmeier, H. Boehnhardt, D. Koschny, E. Kührt and I. Richter, Space Sci. Rev. 128 (2007) 1–21, doi: 10.1007/s11214-006-9140-8.
- J. G. Trotignon, R. Boström, J. L. Burch, K.-H. Glassmeier, R. Lundin,
 O. Norberg, A. Balogh, K. Szegö, G. Musmann, A. Coates, L. Åhlén,
 C. Carr, A. Eriksson, W. Gibson, F. Kuhnke, K. Lundin, J. L. Michau and
 S. Szalai, Adv. Space Res. 24(9) (1999) 1149.
- C. Carr, E. Cupido, C. G. Y. Lee, A. Balogh, T. Beek, J. L. Burch, C. N. Dunford, A. I. Eriksson, R. Gill, K. H. Glassmeier, R. Goldstein, D. Lagoutte, R. Lundin, K. Lundin, B. Lybekk, J. L. Michau, G. Musmann, H. Nilsson, C. Pollock, I. Richter and J. G. Trotignon, Space Sci. Rev. 128 (2007) 629–647, doi: 10.1007/s11214-006-9136-4.
- H. Nilsson, R. Lundin, K. Lundin, S. Barabash, H. Borg, O. Norberg, A. Fedorov, J.-A. Sauvaud, H. Koskinen, E. Kallio, P. Riihelä and J. L. Burch, Space Sci. Rev. 128 (2007) 671–695, doi: 10.1007/s11214-006-9031-z.
- J. L. Burch, R. Goldstein, T. E. Cravens, W. C. Gibson, R. N. Lundin,
 C. J. Pollock, J. D. Winningham and D. T. Young, Space Sci. Rev. 128 (2007) 697–712, doi: 10.1007/s11214-006-9002-4.
- A. I. Eriksson, R. Boström, R. Gill, L. Åhlén, S.-E. Jansson, J.-E. Wahlund, M. André, A. Mälkki, J. A. Holtet, B. Lybekk, A. Pedersen, L. G. Blomberg and the LAP team, *Space Sci. Rev.* 128 (2007) 729–744, doi: 10.1007/s11214-006-9003-3.
- K. H. Glassmeier, I. Richter, A. Diedrich, G. Musmann, U. Auster, U. Motschmann, A. Balogh, C. Carr, E. Cupido, A. Coates, M. Rother, K. Schwingenschuh, K. Szegö and B. Tsurutani, Space Sci. Rev. 128 (2007) 649–670, doi: 10.1007/s11214-006-9114-x.
- J. G. Trotignon, J. L. Michau, D. Lagoutte, M. Chabassière, G. Chalumeau,
 F. Colin, P. M. E. Décréau, J. Geiswiller, P. Gille, R. Grard, T.
 Hachemi, M. Hamelin, A. Eriksson, H. Laakso, J. P. Lebreton, C. Mazelle,
 O. Randriamboarison, W. Schmidt, A. Smit, U. Telljohann and P. Zamora,
 Space Sci. Rev. 128 (2007) 713–728, doi: 10.1007/s11214-006-9005-1.
- L. R. O. Storey, P. Meyer and P. Aubry, A quadripole probe for the study of ionospheric plasma resonances, in *Plasma Waves in Space and in the Laboratory*, (eds.) J. O. Thomas and B. J. Landmark, Vol. 1 (Edinburgh University Press, Edinburgh, Scotland, 1969), p. 303.

- 12. J. G. Trotignon, Short electric-field antennae as diagnostic tools for space plasmas and ground permittivity, in *Advances in Geosciences*, (eds.) A. Bhardwaj *et al.*, Vol. 3, Planetary Science (World Scientific, Singapore, 2006), pp. 71–84.
- 13. J. M. Chasseriaux, R. Debrie and C. Renard, J. Plasma Phys. 8 (1972) 231.
- 14. J. A. Tataronis and F. W. Crawford, J. Plasma Phys. 4 (1970) 231.
- 15. I. B. Bernstein, Phys. Rev. $\mathbf{109}$ (1958) 10.
- 16. B. Rooy, M. R. Feix and L. R. O. Storey, *Plasma Phys.* **14** (1972) 275.
- 17. C. Béghin and E. Kolesnikova, Radio Sci. 33 (1998) 503.
- 18. E. Kolesnikova and C. Béghin, Radio Sci. 33 (1998) 491.
- 19. C. Béghin, Radio Sci. 30 (1995) 307.
- 20. J. Geiswiller, C. Béghin, E. Kolesnikova, D. Lagoutte, J. L. Michau and J. G. Trotignon, *Planet. Space Sci.* **49** (2001) 633.
- J. Geiswiller, J. G. Trotignon, C. Béghin and E. Kolesnikova, Astrophys. Space Sci. 277 (2001) 317.
- K. Hashimoto, W. Calvert and H. Matsumoto, *J. Geophys. Res.* **104** (1999) 28,645.
- J. D. Menietti, R. R. Anderson, J. S. Pickett, D. A. Gurnett and H. Matsumoto, J. Geophys. Res. 108(A11) (2003) 1393, doi: 10.1029/ 2003JA009826.
- 24. N. A. Tsyganenko, Planet. Space Sci. 37 (1989) 5.
- 25. D. L. Gallagher, P. D. Craven and R. H. Comfort, $Adv.\ Space\ Res.\ {\bf 8}(8)$ (1988) 15.
- 26. J. E. Titheridge, J. Geophys. Res. 103 (1998) 2261.